Physica C 498 (2014) 9–13

Contents lists available at ScienceDirect

Physica C

journal homepage: www.elsevier.com/locate/physc

Numerical simulation of mold shape's influence on NbTi cold-pressing superconducting joint

Feng Zhou *, Junsheng Cheng, Yinming Dai, Qiuliang Wang, Luguang Yan

Key Laboratory of Applied Superconductivity, Institute of Electrical Engineering, Chinese Academy of Sciences, Beijing 100190, China

ARTICLE INFO

Article history:
Received 27 September 2013
Received in revised form 16 December 2013
Accepted 22 December 2013
Available online 2 January 2014

Keywords:
NbTi superconducting joint
Cold-pressing welding
Mold shape
Resistance

ABSTRACT

The cold-pressing welding methods are employed to fabricate joints between NbTi multi-filamentary conductors, and a series of joints are made with the molds of different shapes for nuclear magnetic resonance (NMR) magnet applications. The Abaqus–Explicit method was used to do a quasi-static analysis of the cold-pressing welding process. In the simulation, we analyzed four molds with different shapes: plate mold, cap mold, square mold, and radial compression. The simulation shows that the deformation of filaments is the most uniform in the case of radial compression and the square mold is the optimum one for decreasing joint resistance.

© 2013 Elsevier B.V. All rights reserved.

1. Introduction

NMR magnets are important for quality health care. They are very useful in detection and efficient treatment of diseases or injuries. Most of the currently installed NMR magnets are made of NbTi. NbTi joints are inevitable in NMR applications due to the limitation of wire length, and they are always used to connect two adjacent coils [1].

Current-decay rate in the persistent mode operation of NMR magnet is usually determined by the joint resistance [2,3]. The acceptable current decay rate is typically 0.02 ppm per hour when a joint resistance is less than 10^{-11} Ω. To achieve high magnetic field stability in the NMR system, the joints between coils and switches must be fabricated carefully [4].

There are many methods to fabricate superconducting joints, such as, solder welding [5], cold-pressing welding [6,7], and diffusion bonding [8]. Among these methods, the cold-pressing welding method stands out for its convenience and reliability.

Some factors in the pressing process, such as press amount and mold shape, will influence the joint resistance seriously. However, there is no precise instruction on how to choose mold shape until now, which needs to be improved. In this paper, we used Abaqus–Explicit to do a quasi-static analysis of the mold shape's influence on NbTi cold-pressing welding process, which provides certain guiding significance on how to choose mold shape.

The purpose of this research is to improve the cold-pressing welding joint technology: find the influence of different mold shapes—plate mold, cap mold, square mold, and radial compression—on the NbTi superconducting joint and determine which mold benefits mostly for reducing joint resistance.

2. Fabrication method of joints

In practice, the NbTi/Cu wire used to fabricate joints for our NMR magnet is F54 supplied by Oxford Instruments, which has a bare diameter of 0.4 mm, and a Cu/non-Cu ratio of 1.35. The NbTi/Cu tube has a length of 3 cm, external diameter of 4 mm, and internal diameter of 2 mm; the configuration of the cross-section of NbTi/Cu tube is shown in Fig. 1. The cold-pressing welding process includes the following steps:

(I) Remove the insulation layer on wire by abrasive paper.
(II) Remove the stabilizer on the wire by nitric acid until the filaments appear.
(III) Clean the filaments by pure water and ethanol.
(IV) Dry the filaments in open air.
(V) Install the filaments in a NbTi/Cu tube.
(VI) Press the NbTi/Cu tube at a certain press amount in open air with a certain mold.

* Corresponding author. Address: Institute of Electrical Engineering, Chinese Academy of Sciences, No. 6 Beiertiao, Zhongguancun, Beijing, China. Tel.: +86 15801337807.
E-mail address: zhoufeng@mail.iee.ac.cn (F. Zhou).

0921-4534/$ - see front matter © 2013 Elsevier B.V. All rights reserved.
http://dx.doi.org/10.1016/j.physc.2013.12.005

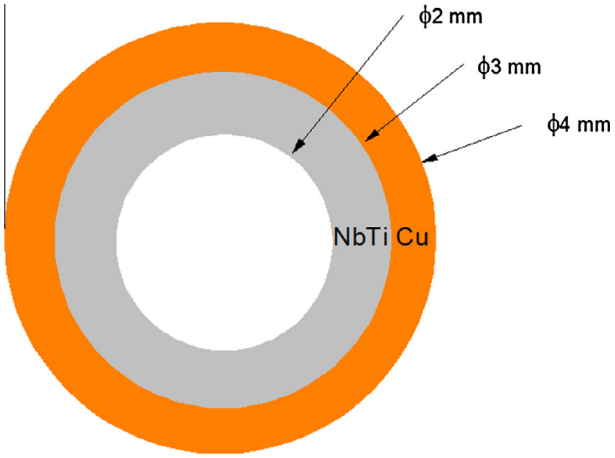

Fig. 1. Schematic cross-section of NbTi/Cu tube.

The press amount is defined as:

$$p = \Delta d/D \times 100\% \quad (1)$$

where Δd is the actual press displacement, D is the possible maximum press displacement. The example before the press operation is shown in Fig. 2.

3. Simulation model

3.1. Analytical model

Four quasi two dimension (2D) finite element (FE) models of the NbTi cold-pressing welding joint were constructed using Abaqus–Explicit. Fig. 3 shows the schematic figures and according parameters of these four analytical models: plate mold, cap mold, square mold, and radial compression. To simplify the model, the Cu layer was ignored, and the external diameter of tube model turned 3 mm. Since NbTi is much harder than Cu, this ignorance will not influence the result seriously. The distribution of filaments is shown in Fig. 3. A fully fixed boundary condition was applied on the die, and displacement boundary condition was applied on the punch. What is worth noting is that, because of the specificity of the case of radial compression, there is not a mold (punch and

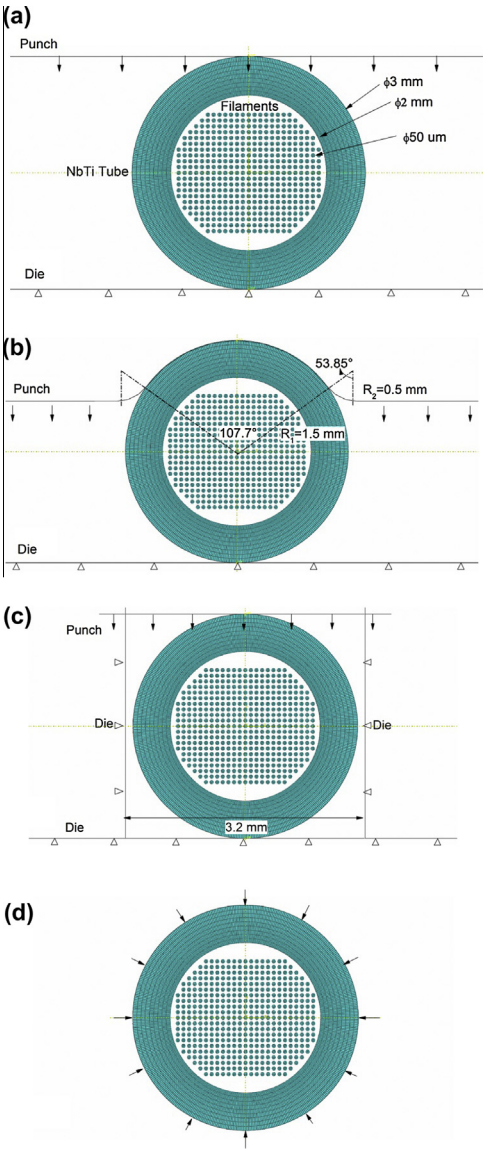

Fig. 3. Parameters of the analytical model, (a) plate mold, (b) cap mold, (c) square mold, (d) radial compression.

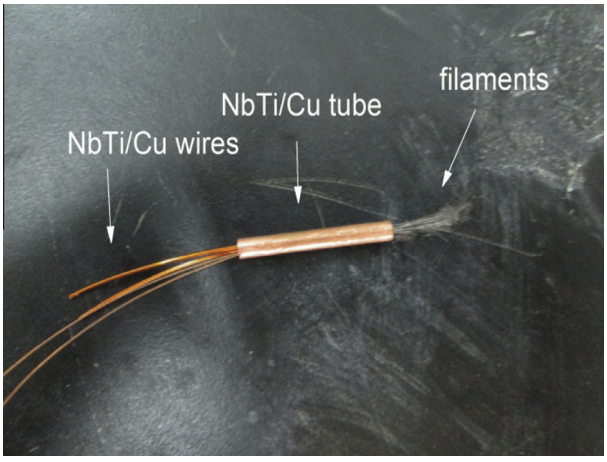

Fig. 2. NbTi joint sample before press operation.

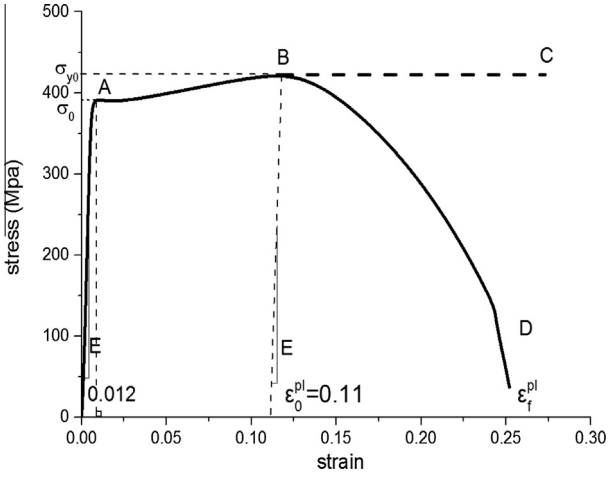

Fig. 4. Stress–strain response curve of NbTi superconductor.

Table 1
Maximum kinetic energy, corresponding internal energy and ratio KE/IE of four models.

Mold shape	Max KE (J)	Corresponding IE (J)	$\frac{KE}{IE}$ (%)
Plate mold	0.0049	0.113	4.33
Cap mold	0.0032	0.103	3.11
Square mold	0.0028	0.187	1.49
Radial compression	0.0062	0.146	4.25

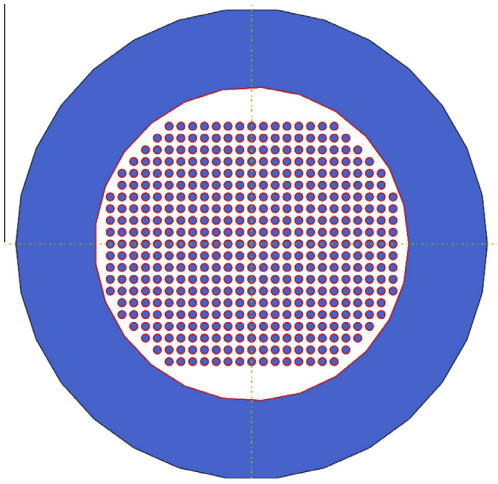

Fig. 5. The definition of contact area (the red region). (For interpretation of the references to color in this figure legend, the reader is referred to the web version of this article.)

die) in the model; in reality, we always use the electromagnetic forming method to fabricate this kind of joints [9].

Contact exists between tube and filaments, and among filaments. A general contact was applied to model the complex contact behavior in the process. A Coulomb friction model was used here. We did an NbTi friction experiment to get the friction coefficient equaling 0.72. 8-noded solid elements (C3D8R) were used for the simulation with 9 element layers through the tube thickness and only 2 element layers through the tube length.

The input to the model consists of NbTi elastic properties and plastic properties. An elastic–plastic tensile experiment of NbTi was carried out. The result of true stress and logarithmic strain is shown in Fig. 4. From Fig. 4, we get: (a) elastic modulus is 60.5 Gpa; (b) NbTi yields at $\varepsilon = 1.2\%$; (c) NbTi begins to damage at equivalent plastic strain $\varepsilon_0^{pl} = 11\%$. Since the stress–strain relationship no longer represents the material's behavior accurately when material necking occurs, an ideal plastic pattern (BC in Fig. 4) is applied in place of the softening branch (BD in Fig. 4) [10]. Poisson ratio, 0.33, is cited from [11]. The density of NbTi, 6027 kg/m^3, can be calculated from the proportion of components Nb 47 wt.% Ti.

3.2. Load

A displacement boundary condition was applied on the punch to press the tube in the model. It is not necessary to define the analysis time as the actual time, since that will make the calculation time too long. We did a quasi-static analysis and defined the analysis time as 0.25 ms to speed up the simulation process. So the punching speed is ~15 m/s in model. The press displacement of punch is applied in a smooth step. Table 1 shows the maximum kinetic energy (KE) and the corresponding internal energy (IE) in the press process of four models. From the ratio KE/IE, we can see that four ratios are all less than 10% (typical threshold) [10]. Hence, according to the energy balance principle, the influence of inertia can be ignored [10], and the analysis time of 0.25 ms is appropriate.

4. Results and discussions

Four models with different press molds were simulated. In the past research, it has been demonstrated that the filaments' contact area and equivalent plastic strain are vital variables to determine the joint's resistance qualitatively—increasing contact is in favor of decreasing joint resistance but increasing strain damage is against that, the lowest joint resistance must be obtained when contact area is large while strain damage is small [12]. It is obvious

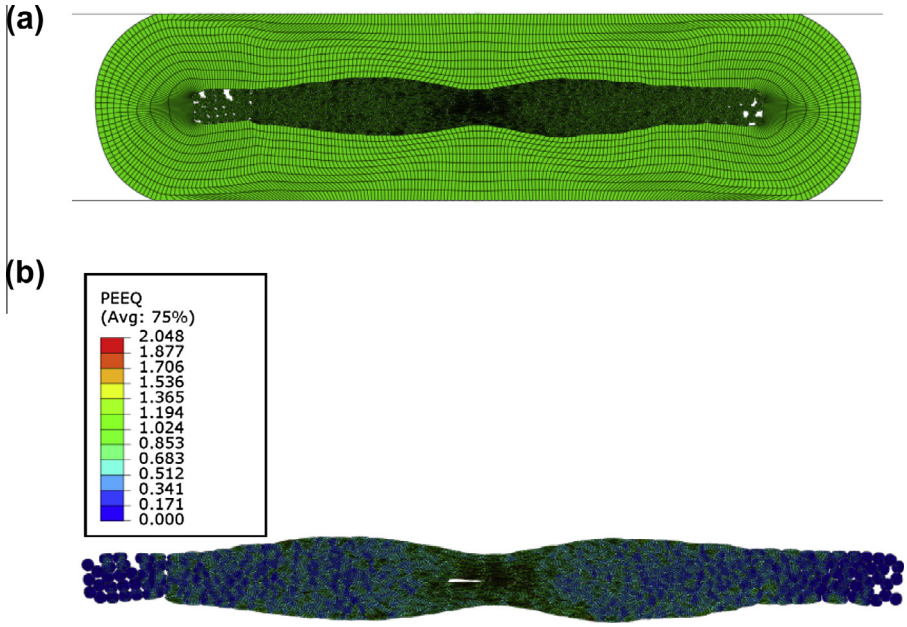

Fig. 6. After press operation, (a) the whole model, (b) filaments' equivalent plastic strain distribution for the case with plate mold.

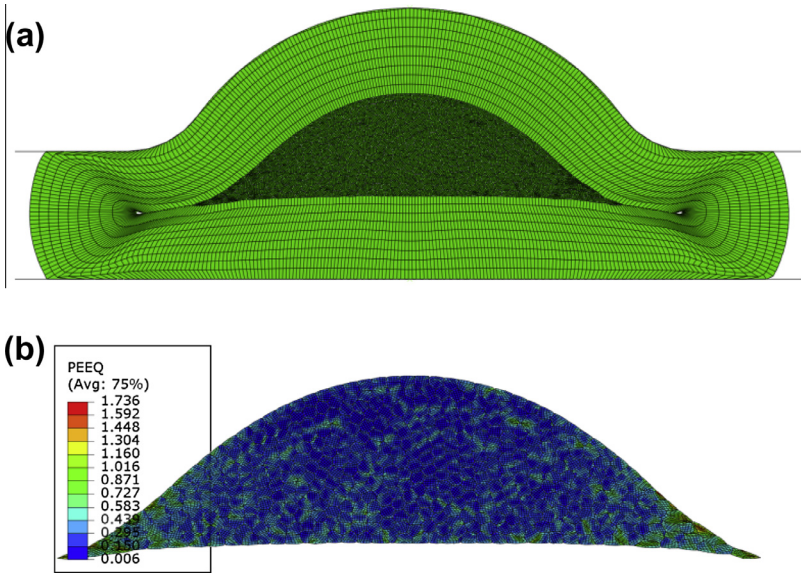

Fig. 7. After press operation, (a) the whole model, (b) filaments' equivalent plastic strain distribution for the case with cap mold.

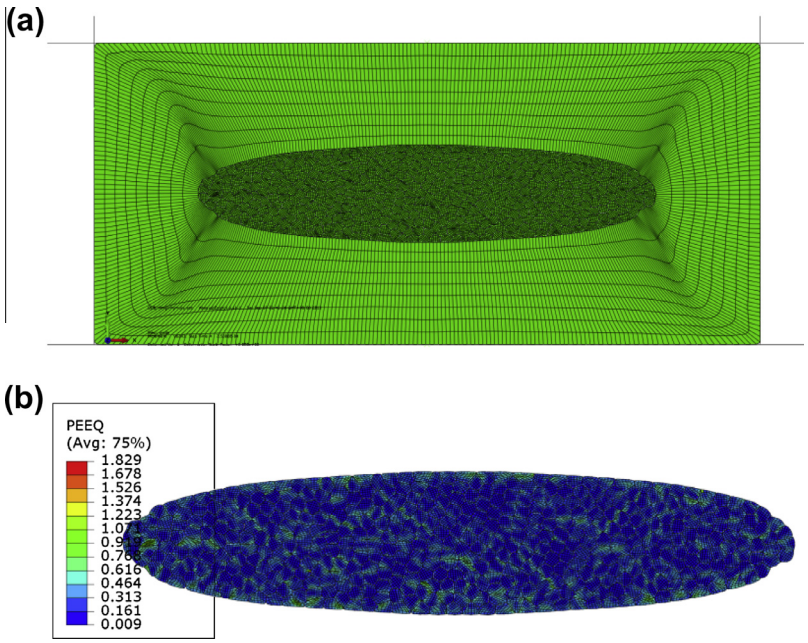

Fig. 8. After press operation, (a) the whole model, (b) filaments' equivalent plastic strain distribution for the case with square mold.

that, as the press amount increases, contact area and strain damage will both increase, but for different press molds, the increasing trends will differ.

The definition of the contact area among filament is shown in Fig. 5 (the red region). Fig. 6 shows the model after press operation and filaments' equivalent plastic strain distribution in the case of plate mold, and Figs. 7–9 shows that of cap mold, square mold and radial compression, respectively.

Comparing Figs. 6(b), 7(b), 8(b) and 9(b), we can find that: (a) the deformation of filaments is the most uniform in the case of radial compression; (b) square mold is also good; (c) for the cap mold, the filaments in the middle region deformed uniformly but the bilateral ones did not; (d) in the case of plate mold, the filaments deformed nonuniformly—the middle region filaments deformed severely while the bilateral ones did not deform at all, even did not contact. Also, we used statistic methods to analyze the variances of the filaments' equivalent plastic strain in the four models, which is shown in Table 2. From Table 2, we can more clearly see the difference of uniformity of filaments' deformation in the four cases—the filaments in the case of radial compression deform more uniformly, then the square mold, then the cap mold, and then the plate mold.

According to the conclusion from the past research [12], we also analyzed the relationship between filaments' average equivalent plastic strain and contact area in the pressing process of four molds, which is shown in Fig. 10, to determine which mold will be the optimum one to fabricate joints with the lowest joint resistance. From Fig. 10, we can see that as contact area increases, the average equivalent plastic strain will also increase, which can be easily understood. However, the increasing trends are different: for the case of plate mold, the average equivalent plastic strain increases the fastest, which means in order to reach the same contact

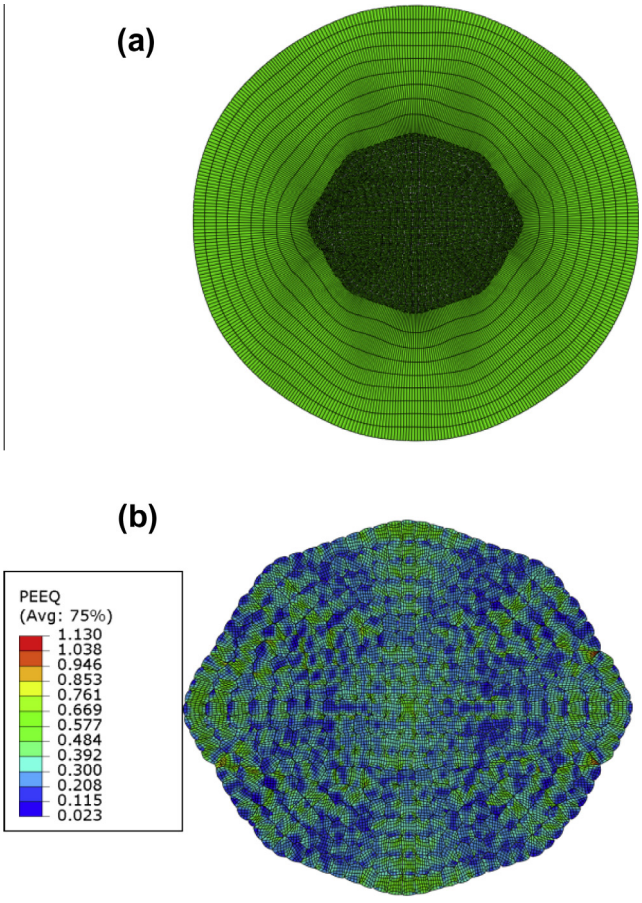

Fig. 9. After press operation, (a) the whole model, (b) filaments' equivalent plastic strain distribution for the case with radial compression.

Table 2
Variances of filaments' equivalent plastic strain of four molds.

Mold shape	Variances of filaments' equivalent plastic strain
Plate mold	0.115
Cap mold	0.040
Square mold	0.027
Radial compression	0.021

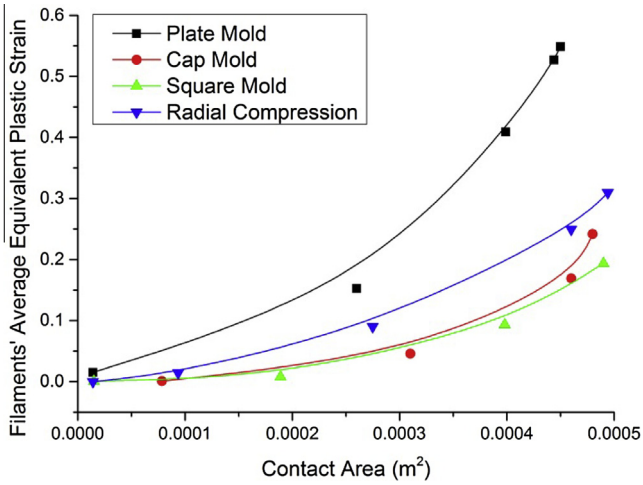

Fig. 10. The relationship between filaments' average equivalent plastic strain and contact area of four models.

area the filaments will deform more severely and thus being easier to damage or even fracture and increase joint resistance; then the radial compression; then the cap mold; and then the square mold. The increasing trends of cap mold and square mold are much similar when contact area is small, but, when contact area exceeds 300 mm^2, cap mold increases much faster than square mold. Because in practice we always want to maximize the contact area, it is concluded that the square mold will be the optimum mold for reducing joint resistance.

5. Conclusions

NbTi cold-pressing welding method is very important for fabricating low resistance NbTi joints for NMR application. This research used Abaqus–Explicit to do a quasi-static analysis of the cold-pressing welding process with four different types of press molds. The simulation results showed that: (a) in terms of the uniformity of filaments' deformation, the deformation of filaments is the most uniform in the case of radial compression, then the square mold, then the cap mold, and then the plate mold; (b) in terms of joint resistance, in the light of the research results in the past, it is concluded that the square mold is the optimum one for decreasing joint resistance in practice.

Acknowledgements

This work was supported by the National Natural Science Foundation of China under Grants 50925726 and 10755001 and by the Instrument Program in MOST.

Appendix A. Supplementary data

Supplementary data associated with this article can be found, in the online version, at http://dx.doi.org/10.1016/j.physc.2013.12.005.

References

[1] Qiuliang Wang, High field superconducting magnet: science, technology and applications, Prog. Phys. 33 (1) (Feb. 2013) 1–23.
[2] C.A. Swenson, W.D. Markiewicz, Persistent joint development for high field NMR, IEEE Trans. Appl. Supercond. 9 (2) (Jun. 1999) 185–188.
[3] Qiuliang Wang, Practical Design of Magnetostatic Structure using Numerical Methods, Wiley, USA, 2013.
[4] P. McIntyre, Y. Wu, G. Liang, C.R. Meitzler, Study of Nb_3Sn superconducting joints for very high magnetic field NMR spectrometers, IEEE Trans. Appl. Supercond. 5 (2) (1995) 238–241.
[5] K. Seo, S. Nishijima, K. Katagiri, T. Okada, Evaluation of solders for superconducting magnetic shield, IEEE Trans. Magn. 27 (2) (Mar. 1991) 1877–1880.
[6] Q. Wang, X. Hu, S. Song, L. Ding, L. Yan, A method for the lower resistance superconducting joints with magnetic field shielded, Patent, ZL201010123276.0.
[7] Junsheng Cheng, Jianhua Liu, Zhipeng Ni, Chunyan Cui, Shunzhong Chen, Shousen Song, Lankai Li, Yinming Dai, Qiuliang Wang, Fabrication of NbTi superconducting joints for 400-MHz NMR application, IEEE Trans. Appl. Supercond. 22 (2) (2012) 4300205.
[8] H.M. Wen, L.Z. Lin, S. Han, Joint resistance measurement using current-comparator for superconducting wires in high magnetic field, IEEE Trans. Magn. 28 (1) (Jan. 1992) 834–836.
[9] Q. Wang, X. Hu, J. Cheng, L. Yan, H. Wang, C. Cui, Electromagnetic forming for the superconducting joints, patents, Cn 201210278270.X.
[10] Dassault, Abaqus Analysis User's Manual, Abaqus 6.11, Champs Elysees, France, 2011.
[11] Wei Qinwei, Hu Jishi, Dong Liang, Yan Zhongming, Zhu Yingwei, Wang Yu, Electromagnetic-structural coupling analysis of the pulse superconducting magnet based on ANSYS, Sci. Technol. Eng. 15 (2009) 4395–4397.
[12] Feng Zhou, Junsheng Cheng, Jianhua Liu, Yinming Dai, Qiuliang Wang, Namin Xiao, Luguang Yan, Numerical simulation of NbTi superconducting joint with cold-pressing welding technology, IEEE Trans. Appl. Supercond. 23 (6) (2013) 4802706.